

AN OPERATIONAL SEDIMENT FLUSHING SCHEME FOR THE OCAÑA HYDROPOWER PLANT REGULATION RESERVOIR IN ECUADOR

OSWALDO TORRES^{*(1,3)}, PEDRO D. BARRERA^{*(1,3)} & MARCELO H. GARCIA⁽²⁾

⁽¹⁾IAHR Member, Facultad de Ingeniería en Ciencias de la Tierra, Escuela Superior Politécnica del Litoral, Ecuador

⁽²⁾IAHR Member, Ven Te Chow Hydrosystems Laboratory, Department of Civil and Environmental Engineering, University of Illinois at Urbana - Champaign, USA

⁽³⁾IAHR Member, HIDRODICON, Ecuador

*Both authors contributed equally to this manuscript

cotorresv@gmail.com; pdbc.1985@gmail.com; mhgarci@illinois.edu

ABSTRACT

The Ocaña hydropower plant in Ecuador has been affected by long shutdowns related to sediment accumulation in its regulation reservoir. The lack of sediment flushing strategies has caused the plant to operate, in several occasions, under severe sedimentation levels that greatly hinder the maintenance and cleaning of the reservoir. In that regard, a specific definition of how and when to evacuate the sediment is needed. Therefore, a process-based numerical model was implemented to reproduce the hydrodynamics and morphodynamics inside the structure, and evaluate different sediment flushing operations. The proposed schemes make use of the available gates and sluices that are already a part of the plant's intake and regulation system infrastructure. Moreover, to determine the respective sedimentation rates and loss of storage volumes during continuous plant operation conditions, the morphological evolution of the bed was forecasted until the level of siltation reached its maximum. Results show that the most efficient sediment flushing strategy allows water to enter via the river intake while the reservoir is being emptied through the flushing gate. Additionally, the model shows that by carrying out periodic sediment flushing operations every 2 months, the need to perform complete cleanings of the structure would be limited to only twice a year, which would greatly enhance the power plant operation.

Keywords: hydropower; sedimentation; process-based numerical model; morphological evolution forecast, sediment flushing.

1 INTRODUCTION

In the past, sedimentation management was a parameter not considered during the design and construction of reservoirs (Garcia, 2008). According to the earlier work by Brune (1953), 90% of the incoming sediment load is trapped in most regulation reservoirs. Nowadays, many analytical and numerical models have been developed (Dam et al., 2016; Giardino et al., 2014, 2018; Savenije, 2006; Van der Wegen and Roelvink, 2012; Van Rijn, 2011; Winterwerp, 2013) in order to acquire knowledge about the water and sediment interaction, to quantify the physical processes in reservoirs (Hoitink et al., 2017), and to optimize and increase the design life and operability of the structures affected by particles settling along a given reservoir (Morris et al., 2008).

In reservoirs for small power plants, the sediment accumulation and the consequent loss of volume determines the generation capacity during hours of peak demand. Moreover, the sediment that enters the conveyance system contributes to the wear and tear of the hydromechanical equipment, such as the turbine runner. In this regard, sediment control strategies that involve hydraulic methods have been introduced to route the material out the reservoirs and mitigate the volume loss. Fan & Morris (1992) describe the classic methods that include sediment sluicing (drawdown routing), drawdown flushing and venting of density currents. Among these methods, drawdown flushing (hereafter referred to as sediment flushing), is the most common approach implemented in reservoirs at small hydropower plants in Ecuador. Often this operation requires the total shutdown of the plant. It also involves the complete drawdown of the reservoir water level in order to generate a high velocity flow that is able to erode existing deposits. Most of the eroded material is limited to a flushing channel that can only liberate some of the storage volume. As a consequence, the sediment outside the eroding zone of the flushing channel has to be removed mechanically using heavy machinery. Depending on the rate of sedimentation and degree of consolidation attained, the total cleaning of the reservoirs can take days up to weeks to be completed. This causes not only higher maintenance and operational costs but also results in lost profits due to the plant shutdown and lack of energy production.

This study uses a process-based numerical model to reproduce the morphodynamic evolution, during a flushing operation, of the deposited sediment in the Ocaña hydropower plant regulation reservoir. Since its commissioning in 2012, the plant has experienced long shutdowns ascribed to the sedimentation in the reservoir. The cohesive nature of the deposits makes the maintenance and clean-up tasks extremely difficult. Besides, the loss of active storage volume under severe sedimentation, makes the plant generation capacity vulnerable. In that regard, an improvised operational scheme has been implemented in which the total removal of sediment is conducted 6 times a year (Montesdeoca, 2018). However, this operational scheme is based largely on the judgment of the operators to schedule the cleaning. Therefore, the aim of the current research is to implement a model of the reservoir in order to propose new operational rules that provide clear guidelines to suggest how and when to implement the flushing of sediments. Based on the suggested new rules, the objective is to improve the efficiency of the flushing operation and to limit the maintenance and plant-shutdown durations.

1.1 Study area

Ocaña is a run-of-the-river hydropower plant located at 845 meters above mean sea level (AMSL), and 25Km from the village of Cochancay, in the rural parishes of the Cañar Province in the southwestern part of Ecuador. The plant's intake structures are designed to conduct a flow of $8.20 \text{ m}^3/\text{s}$ from the Cañar River to the power house. The diverted water moves two vertical axis Pelton turbines that are able to generate approximately 26 MW of power.

The layout of the intake and regulation systems, displayed in Figure 1, describes the lay-out of the structures. Water entering through the river intake passes through a gravel trap, the sedimentation chamber followed by the by-pass tank prior to its arrival at the regulation reservoir. Throughout this path, the main function of the structures mentioned, with the exception of the by-pass tank, is to remove the largest amount of solid material that is transported by water such as gravel, sand and suspended silt. The by-pass tank provides the possibility to operate the plant temporarily while maintenance and cleaning of the regulation reservoir is carried out. This tank is connected to the head race tunnel by means of a by-pass pipeline.

Water inside the reservoir ultimately flows towards the forebay. The forebay is built directly on the shortest side of the reservoir, and is connected to the headrace tunnel by a low-pressure pipeline (1.90 m inner diameter). Finally, the reservoir flushing gate is located to the left of the forebay. The gate is 2m wide by 2 m high, and gives way to the flushing channel which discharges directly back towards the Cañar River during flushing operations.

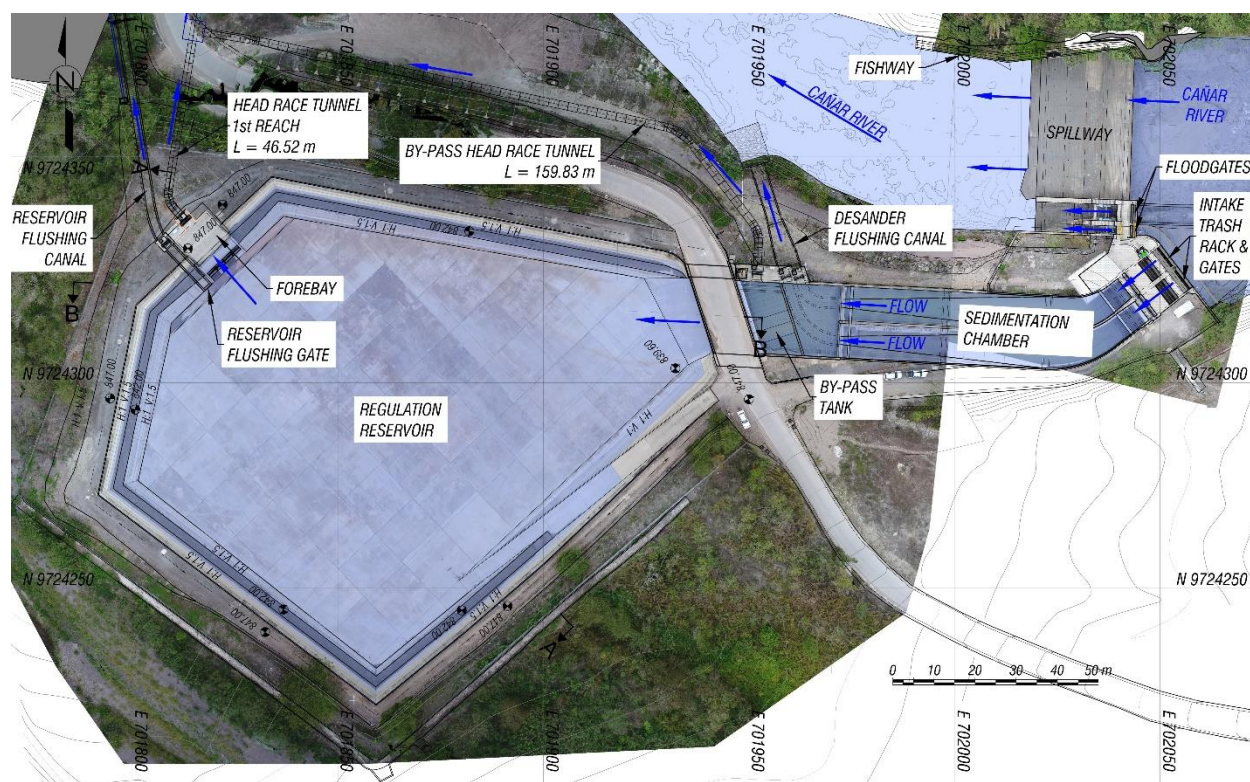


Figure 1. Intake and regulation system layout of the Ocaña hydropower plant in Ecuador.

1.2 Regulation reservoir

The reservoir has a pentagonal shape and covers an area of 1.24 Ha that is completely lined with concrete. The water enters through the western side of the structure. The design is based on securing the plant's power generation by storing water during low-demand hours and using the additional volume during peak-demand hours. According to Caminosca (2008a), the plant has a daily independence time of 3 hours of generation using the water in the active storage volume. In summary, the reservoir has a total volume of 95658.29 m³, which is located between 847.00 AMSL and 836.54 AMSL and includes

- Dead storage volume (22228.52 m³), which is located below the level 840.50 AMSL and is thought to store the sediment that deposits during normal operation of the plant.
- Active storage volume (44653.67 m³), located between 844.60 AMSL and 840.50 AMSL. It contributes to the power generation according to the demand pattern.
- Emergency storage (28776.10 m³), which is used in case that there is no water inflow from the river during the operation of the plant. It is located between levels 847.00 AMSL and 844.60 AMSL.

2 MATERIALS AND METHODS

2.1 Data collection

The data collection was focused on determining the main characteristics under which the plant operates during reservoir flushing operations, as well as the boundary conditions and some of the necessary hydraulic and morphological parameters for the subsequent implementation of a numerical model.

The following data types were collected and processed before being used as input to the numerical model: geometry of the hydraulic circuit between the river intake and the forebay, evolution of the reservoir's bed topography in the time period elapsed between consecutive flushing operations, water levels and discharges in the reservoir, and characteristics of the deposited sediment.

The geometry of the hydraulic circuit stemmed directly from the as-built documents of the plant. Moreover, through the analysis of a chronological series of bathymetries, carried out over a period of 4 months of uninterrupted plant operation, the evolution of the reservoir's bed topography was assessed.

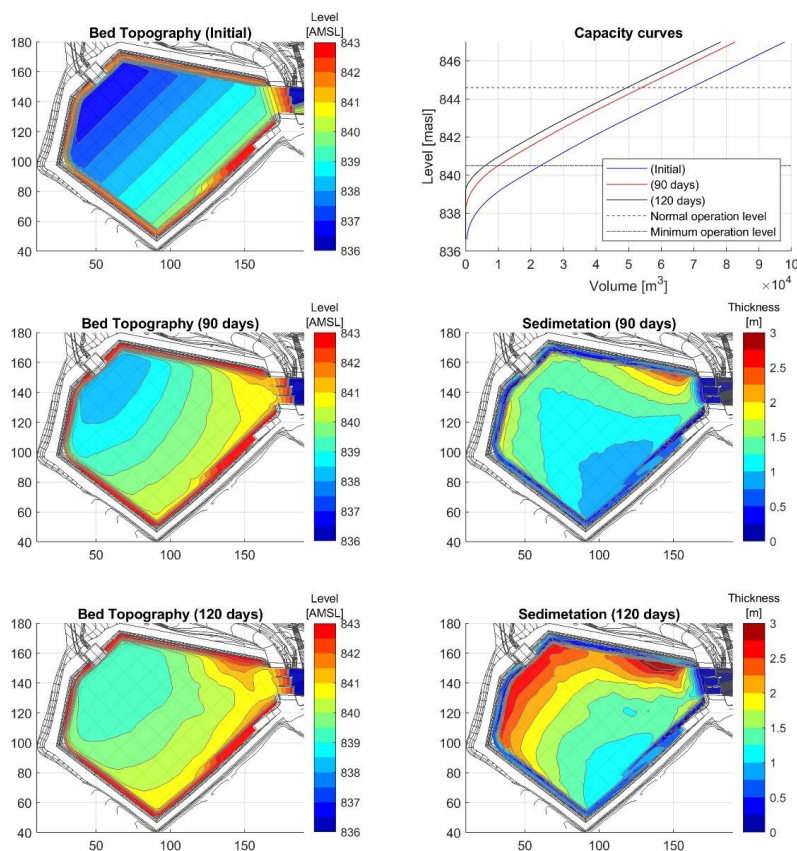


Figure 2. Bed topography and sedimentation patterns measured in the regulation reservoir after 90 and 120 days of uninterrupted plant operation.

A total of 3 bathymetric surveys were carried out. The first one was done after a total cleanup of the reservoir. The main objective was to determine with precision the initial condition, and to corroborate the detailed information in the as-built documents of the structure. The second and third surveys were carried out after 90 and 120 days respectively. The plots on the left of Figure 2 show the results of each of the bathymetric surveys. Levels are shown with contour lines every 0.50 m for each case. The two lower graphs on the right side of Figure 2 show the sedimentation patterns reached in each case. These patterns express the depth of the sediment layer deposited on the bottom. Additionally, the upper right plot presents the capacity curves for each instance. The curves indicate the volume of water as a function of the bottom sediment levels. The minimum and normal operational levels are also shown as reference in the same plot. In order to characterize the sediment, a total of 6 samples collected during the bathymetric surveys were analyzed. The material was defined as fine grained, cohesive sediment (clay) with high water content, which was not consolidated. In that regard, the mean grain size D_{50} was estimated as $12.30 \mu\text{m}$, and the dry-bulk density was 452.72 kg/m^3 .

The sedimentation patterns in Figure 2 show that at the beginning of the morphological development the zone located towards the northern side of the reservoir is the most susceptible to sedimentation. The sediment layer around this area reaches 2 m and 3 m at 90 and 120 days, respectively. Additionally, it can be deduced that the deeper zones are also prone to sedimentation. Consequently, the morphological evolution of the bed is such that the deeper areas are gradually leveled with the most superficial areas. As time passes, this results in a topography of the bed that renders a fairly uniform level throughout the bottom of the structure. After 90 days the reservoir's volume is reduced by approximately 13270 m^3 , and after 120 days the reduction reaches 17740 m^3 . Although the sedimentation rate is not constant, on average the volume loss is about $4423 \text{ m}^3/\text{month}$.

2.2 Current flushing operation of the regulation reservoir

The flushing of the reservoir is an operation that is carried out in 2 stages:

- The river intake gates are closed and the plant continues to operate normally until the water level in the structure reaches the minimum operating level (840.50 AMSL). At this time, the plant operation continues by using water from the by-pass tank.
- Once the minimum operation level is reached, the penstock intake gates are closed and the flushing gate of the reservoir is opened. The complete opening is accomplished after 5 minutes. Finally, with the fully opened flushing gate, the water is discharged directly to the Cañar River.

Figure 3 shows the variation of the water level within the reservoir as well as the flow rates that are discharged through the forebay pipeline and through the purge gate during the flushing operation. The total duration of the maneuver lasts around 2 hours. During the first stage it can be observed that the water level drops on average at a rate of 0.04 m/s and the minimum level of operation is reached in approximately 90 minutes. The water level descent is much faster during the second stage, since the discharge capacity of the purge gate is greater. Total emptying during the second stage occurs in about 30 minutes.

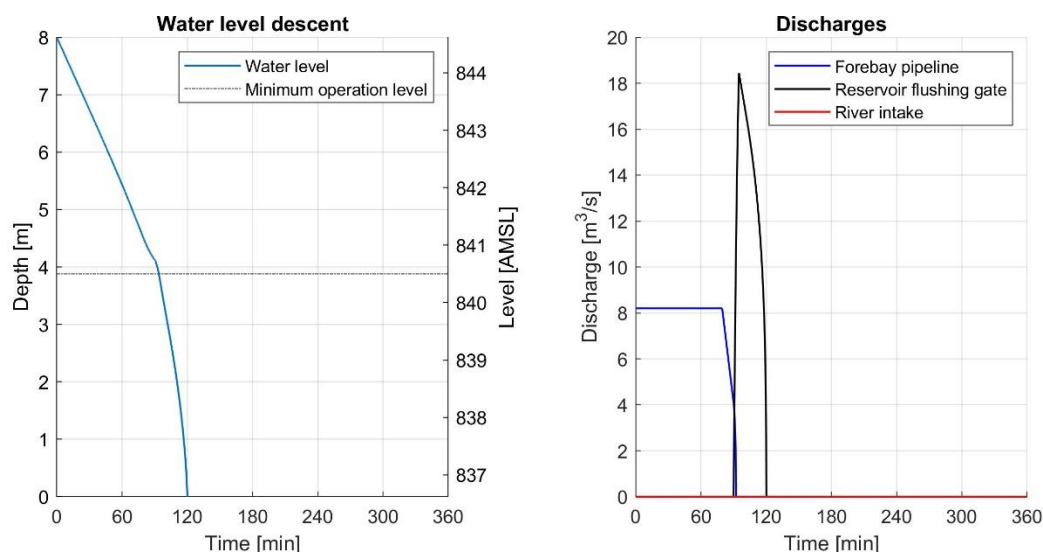


Figure 3. Water level descent and discharges during the current forebay flushing operation.

2.3 Numerical model

The process-based Delft3D model was used to simulate the coupled hydrodynamics, sediment transport and morphodynamic processes in the reservoir. Delft3D solves the two- and three-dimensional shallow water equations on a structured grid, based on the finite-differences method (Deltares, 2014).

The model domain covers the entire structure from the by-pass tank up to the forebay intake gates (Figure 1). The grid resolution ranges between 0.50 m and 2.00 m in the denser areas, and from 2.00 m up to 5.00 m in the areas toward the edges of the structure. Prior to the start of the flushing maneuver, the reservoir is considered to operate under normal conditions (water level is taken at 844.60 AMSL). The flow boundary conditions are given by the discharges through the river intake, the forebay pipeline, and the reservoir flushing gate. Moreover, the bed level at the boundaries is considered fixed so that no morphological changes occur. Based on the field measurements, a uniform fine sediment fraction is defined. Given the cohesive nature of the sediment, the fluxes between the water column and the bed are calculated with the Partheniades-Krone formulation (Partheniades, 1964).

The main parameters for the hydrodynamic and the morphodynamic modules of the model are listed in Table 1. The parameters related to the sediment characteristics were obtained directly from the field measurements and the rest are obtained during calibration of the model.

Table 1. Input model parameters.

DESCRIPTION	PARAMETER	UNIT	VALUE
Spiral flow intensity	β	[-]	0.50
Turbulent background horizontal eddy viscosity	ν_H	[m ² /s]	0.10
Turbulent background horizontal eddy diffusivity	D_H	[m ² /s]	0.15
Manning friction coefficient	n	[s.m ^{-1/3}]	0.03
Sediment specific density	ρ_{sed}	[kg/m ³]	2650.00
Mean sediment diameter	D_{50}	[μ m]	12.30
Dry bed density	ρ_{dry}	[kg/m ³]	452.72
Sediment settling velocity	ω_s	[mm/s]	0.36
Critical bed shear stress for erosion	τ_e	[Pa]	2.03
Critical bed shear stress for sedimentation	τ_s	[Pa]	1000.00
Erosion parameter	M_s	[kg.s/m ²]	0.046

2.4 Schematization of the different cases

Normally, a hydraulic flushing of the regulation reservoir is done prior to the complete cleaning of the structure. The total cleaning is a laborious and extensive job that involves the use of heavy machinery to remove the accumulated material, and the total shutdown of the plant, without energy generation. The duration of the plant shutdown depends on the degree of sedimentation attained at the time of the flushing (it is reported that under the current operational practices, it takes about 2 to 5 days to clean the reservoir completely). Moreover, the greater the amount of sediment allowed to accumulate, the greater the potential repercussion on water quality that a sudden sediment-laden discharge into the river may cause. That is why it is desired to reduce the frequency of total cleanings as much as possible. Consequently, it is necessary to identify an operational scheme in which the action of the hydraulic flushing is maximized. The idea is that by carrying out sediment flushing more frequently, the time between the complete cleanings of the reservoir can be extended.

Based on this reasoning, the maneuvers described below consider the use of the gates available in the hydraulic circuit such as: the river intake gates, the forebay gate that controls the entry of water to the headrace tunnel, and the reservoir flushing gate.

- **Maneuver 01:** This maneuver describes the current reservoir flushing practice shown in Figure 3. That is, the river intake gates are closed and the plant continues to generate power until the water descends to the minimum operational level. From this point, the purge gate is opened and all the remaining water is discharged directly into the river downstream.
- **Maneuver 02:** This maneuver takes advantage of the river intake capacity to allow the entry of water while the emptying is carried out through the flushing gate. Once the minimum level has been reached by generation, the flushing gate opens. The moment in which this gate is completely open, water is allowed to enter from the river intake by opening only one of the two available intake sluices. That is,

during the purge, the entry of $4.10 \text{ m}^3/\text{s}$ is allowed from the intake. The plots of Figure 4 show the variation of the respective water levels and discharges.

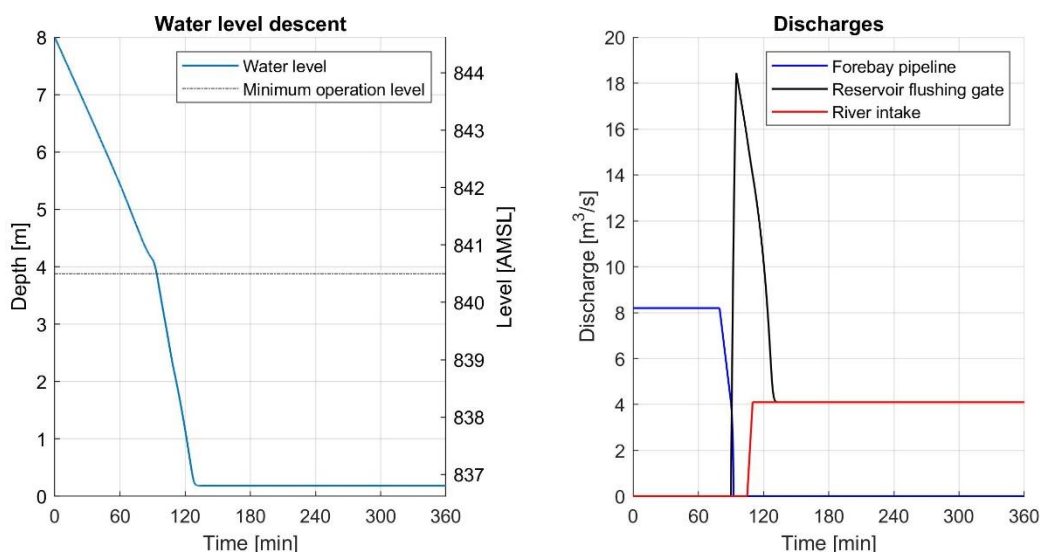


Figure 4. Water level descent and discharges during the **Maneuver 02** flushing scheme.

- **Maneuver 03:** This flushing scheme is similar to the previous one with the difference that it allows the entry of a larger flow from the river intake during the purge ($8.20 \text{ m}^3/\text{s}$). For this, the two intake sluices are opened simultaneously. Figure 5 shows that by implementing this maneuver, the rate of descent of the water level decreases, which causes the flow during the flushing to be maintained for a longer time in relation to the previous cases.

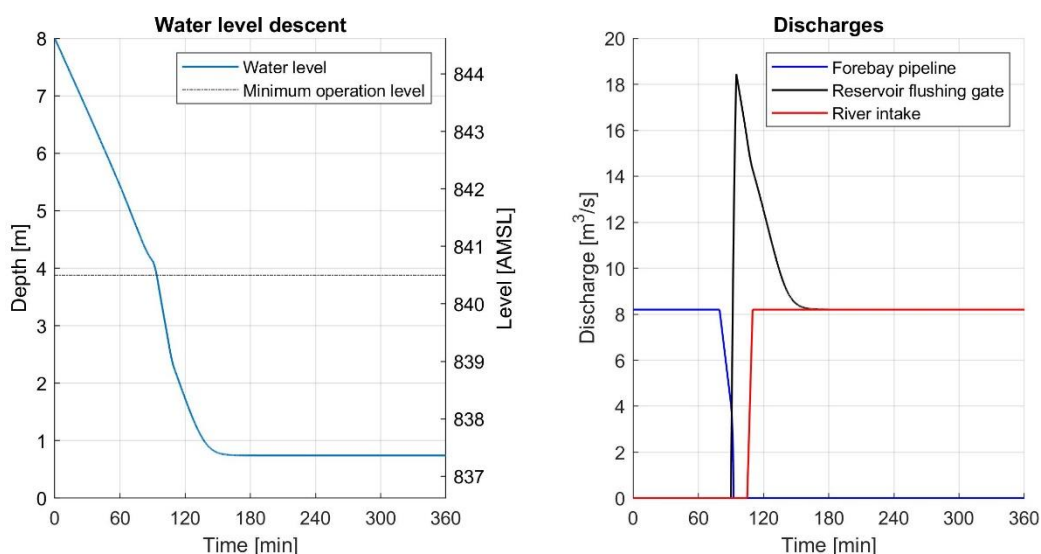


Figure 5. Water level descent and discharges during the **Maneuver 03** flushing scheme.

3 RESULTS

3.1 Calibration and validation

The calibration was carried out by tuning the parameters shown in Table 1 related to bed level friction (Mannig et al., 1890), the turbulence closure model and the constants in the sediment resuspension and deposition formulation. Starting from a situation depicting the reservoir completely clean, the objective was to adjust these parameters until the model is able to reproduce the sedimentation patterns measured after 90 days of uninterrupted plant operation. To avoid subjectivity in the interpretation of the results, the predictive capability of the model was evaluated using the Brier Skill Score index (BSS) (Sutherland et al., 2004; Van Rijn et al. 2003), which has been specially defined for morphodynamic studies. After the calibration exercise, the obtained

BSS was 0.87 which, according to the classification posed by Van Rijn et al. (2003), corresponds to an excellent prediction.

The validation follows a similar methodology. With the optimum set of parameters, a model prediction was performed aimed at reproducing the sedimentation patterns after 120 days. After comparing the measured and modelled results, the respective BSS was 0.83, which is also deemed as an excellent representation.

3.2 Evolution of water and sediment volumes inside the regulation reservoir during normal plant operation

Prior to the analysis of the flushing operations, a projection of the evolution of the volumes inside the reservoir (dead storage, active storage and overall water and sediment volumes) was made with the aid of the model. The projection assumes a continuous operation of the plant under design conditions and the average measured annual sediment input from the river. The aim was to monitor the development of the volumes inside the reservoir until the maximum level of siltation occurs.

The left plot in Figure 6 shows how the volumes change inside the reservoir. As sedimentation progresses, the dead storage decreases at a higher rate and becomes fully occupied by sediment after 270 days. At this instance the active storage has also been reduced by about 30% of its initial volume (44653 m³). During this time the sedimentation rate is fairly constant and can be estimated to be 4400 m³/month, which agrees with the estimated sedimentation rate measured during the field data collection campaign. Afterwards, the sedimentation rate decreases until the point where the complete siltation of the reservoir occurs at 510 days. The right plot from Figure 6 shows the situation with the reservoir full of sediment. A channel-like path is formed in the deposited material where water flows directly from the reservoir's water entry towards the forebay, and little to no additional sedimentation occurs. This situation was actually observed prior the first total cleaning of the reservoir in 2014 after the plant operated continuously for over 2 years (Montesdeoca, 2018).

A closer examination of the active storage curve during the first months of operations reveals that around 120 days (i.e., when the active volume reaches 63% of the initial total storage volume or when the sediment volume reaches 16750 m³) the volume decreases at a constant rate. Afterwards, the volume loss accelerates notably due to the almost depleted dead storage. Hence, this point can be defined as the threshold from which a total cleaning of the reservoir is needed.

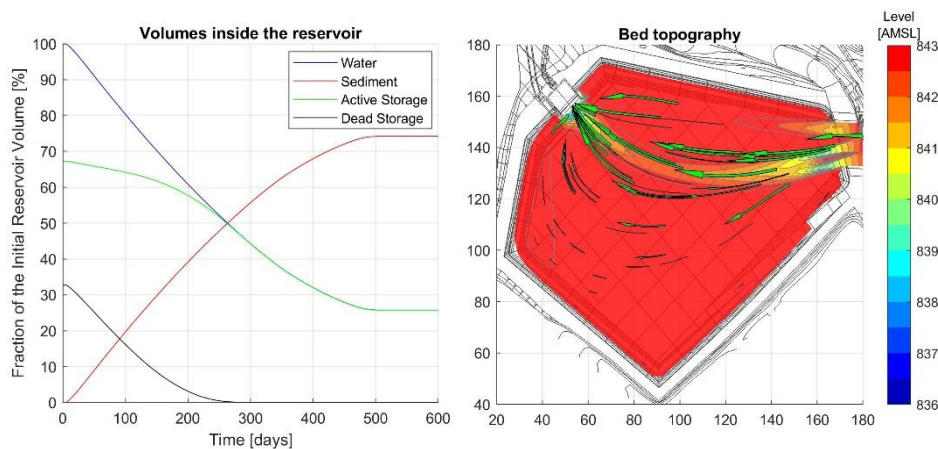


Figure 6. Water and sediment evolution volumes inside the reservoir (left). Predicted bed topography after 18 months of continuous plant operation (right) (green vectors depict the flow of water over a period of 10 minutes).

3.3 Morphological evolution of the deposited sediment during the proposed flushing operation schemes

For the evaluation of each one of the 3 flushing maneuvers described, the corresponding simulations were carried out with the numerical model. The strategy was to evaluate the sediment purge capacity of each maneuver as a function of the degree of sedimentation reached at the end of continuous plant operation periods established in 30, 60, 90 and 120 days.

To avoid redundancy, Figure 7 shows the predicted bed levels after each maneuver is finished only for the case associated to the sedimentation reached at 120 days of continuous plant operation.

In relation to **Maneuver 01**, it is observed that the bed topography remains almost unchanged except for the zone at the vicinity of the reservoir's flushing gate. During the operation, around this area, the velocity field converges rapidly and the greatest sediment transport occurs. This indicates that the sediment purge capacity is a function of both the magnitude of the flow velocity that may occur and the time during which a flow is actually present. In summary, the purge action of the emptying maneuver is focused exclusively around the flushing gate.

The morphological evolution during **Maneuver 02** occurs as a retrogressive erosion of the bed in the northern part of the reservoir (just where the greatest degree of sedimentation occurs during normal plant operation). This erosion begins by delineating a well-defined path between the entrance to the reservoir and the flushing gate. The width of this path increases as the flow erodes the deposited material. Depending on the degree of sedimentation achieved, prior to the execution of the maneuver, the erosive action of the flow allowed through the intake gate is able to completely or partially clean the sediment along the north face of the reservoir.

Maneuver 03 presents similar results to the previous case. The formed erosion channel tends to be oriented slightly more towards the southern part. Thus, the sediment removal reaches deeper areas. As stated before, the degree of sedimentation dictates the extent of the erosive action of the flow entering the river intake gates.

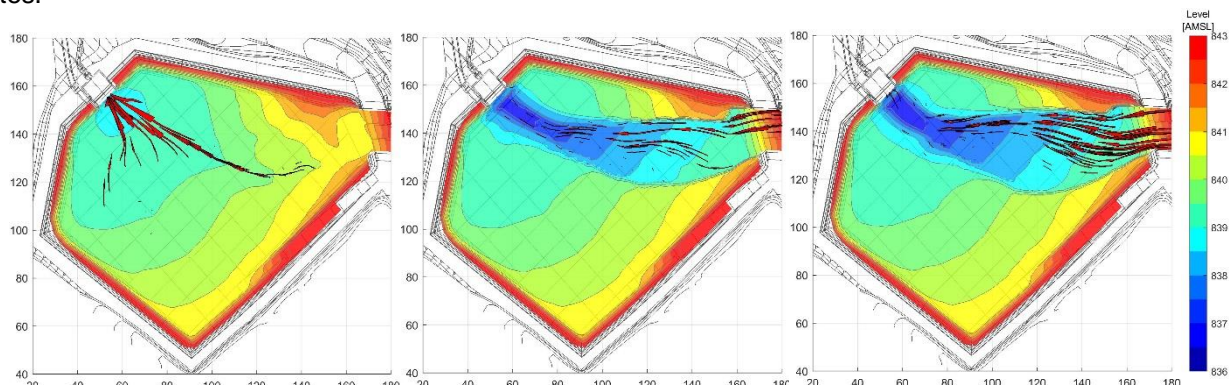


Figure 7. Predicted bed topography at the end of the proposed flushing operations: **Maneuver 01** (left), **Maneuver 02** (center), **Maneuver 03** (right) (red vectors within the flow pattern depict the flow of water over a period of 10 seconds).

3.4 Sediment removal efficiency of the proposed drawdown flushing schemes

The top plots of Figure 8 display the volume of sediment purged for each situation. As expected, **Maneuver 03** is the one that removes the largest amount of material. For the 90 and 120 days of sedimentation cases, a sudden increase in the purged sediment volume is produced approximately at 4.5 hours from the start of the operation; i.e., 3 hours from the opening of the flushing gate. This can be attributed to the bank erosion that occurred along the formed channel the moment it reaches the deepest areas in the reservoir.

The flushing efficiency ($\eta_{Flushing}$) is defined as the ratio between the purged sediment volume and the initial sediment volume accumulated in the reservoir prior the execution of the flushing maneuver. The bottom plots of Figure 8 show the flushing efficiency for each scenario. The results for **Maneuver 03** confirm that it is clearly the most efficient one. However, the efficiency is reduced as the amount of sediment within the reservoir increases. Thus, after 120 days the efficiency is less than half the values obtained at 30 days. This indicates that even though more sediment can be evacuated at the end of longer periods of continuous plant operation, this is not an efficient practice. Instead, by increasing the frequency of hydraulic flushing, the erosive action of the flow will target the zone around the northern side of the reservoir, which is the most prone to sedimentation. As a consequence, the periods between complete cleanings of the reservoir can be extended.

With respect to the time required for the flushing operation to be conducted, it can be seen that approximately after 4 hours from the start, the efficiency increases at a lower rate. This indicates that from this point on, the purged sediment does not increase and the duration of the maneuver can be limited to 4 hours.

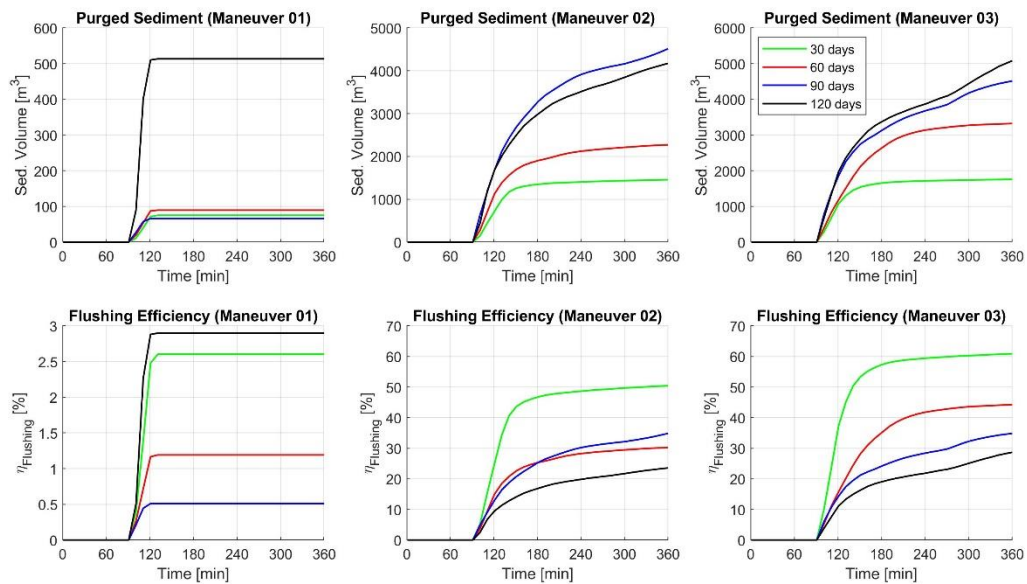


Figure 8 Flushing efficiency and volumes of sediment evacuated during the proposed operations: **Maneuver 01** (left), **Maneuver 02** (center), **Maneuver 03** (right).

3.5 Annual program of flushing and cleaning operations of the regulation reservoir

Based on the average sedimentation rate under normal plant operation, the threshold volume that defines when a total cleaning is needed and the sediment volumes evacuated with **Maneuver 03**, the frequency of its execution can be determined.

Figure 9 shows, within an annual context, the frequency with which total cleanings must be carried out in case of performing periodic hydraulic flushing every 30, 60 and 90 days. It can be noted that for the cases when hydraulic flushing is performed every 30 and 60 days, a total of 2 complete cleanings per year are required. On the other hand, if hydraulic flushing is carried out every 90 days, a total cleaning is required every 5 months. It can then be concluded that the best maintenance practice is to perform periodic flushing operations every 2 months. In this way, a total cleaning of the regulation reservoir will be needed every 6 months.

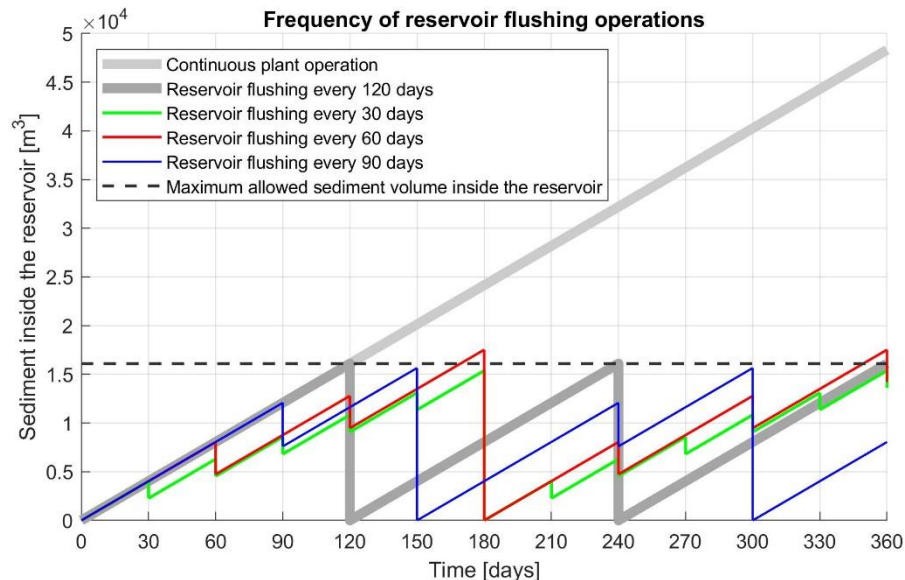


Figure 9. Yearly schedule of flushing operations and total cleaning of the regulation reservoir.

4 CONCLUSIONS

The present research describes the application of a hydromorphodynamic process-based model to the Ocaña hydropower plant regulation reservoir, where different drawdown flushing operations schemes for sediment management strategies are analyzed. The main goal was to improve the reservoir efficiency and to define guidelines to implement a maintenance strategy, and to increase the time between a total removal of sediments.

The model was properly calibrated and validated against field measurements that were carried out as a part of the investigation.

A prediction of the volumes inside the reservoir was carried out with aid of the model. It was found that after 270 days, the dead storage becomes fully occupied by sediment, and the active storage is reduced by about 30% of its initial volume. During this time the sedimentation rate is fairly constant, after which it decreases until the reservoir is fully occupied which occurs at 510 days. Additionally, a limit for a total cleaning of the reservoir was found, based on the point at which the active volume reaches 63% of the initial storage volume, and the active storage curve starts to decrease at a constant rate.

Three maneuvers were proposed as drawdown flushing operations schemes. It was found that by executing sediment flushing operations every 2 months, according to the **Maneuver 03** scheme, the need to perform a total cleaning of the reservoir is reduced to twice a year. This approach will reduce the plant shutdowns related to sediment removal to about a third of the time required by current practices.

ACKNOWLEDGEMENTS

The authors would like to thank Antonio Borrero, General Manager of Electro Generadora del Austro S.A. (ELECAUSTRO S.A.), and all the staff that is in charge of the operation and maintenance of the Ocaña Hydropower Plant. We would like to especially thank Sebastián Montesdeoca, who closely monitored the development of this research, facilitated information gathering and allowed the access to facilities and equipment during the field investigations. The results and conclusions presented above are exclusive to the authors and do not represent the opinion of any agent.

REFERENCES

- Ariathurai, R., & Arulanandan, K. (1978). Erosion rates of cohesive soils. *Journal of the hydraulics division*, 104(2), 279-283.
- Brune, G. M., Trap Efficiency of Reservoirs. *Transactions of the American Geophysical Union*, Vol. 34, No. 3, June, 1953, pp. 407-448.
- CAMINOSCA (2008a). Estudios de Factibilidad y Diseños Definitivos del Proyecto Hidroeléctrico Ocaña - Etapa de Factibilidad - Anexo No. 1 - Hidrología. *Technical report*. CAMINOSCA C. LTDA.
- Dam, G., Van der Wegen, M., Labeur, R. J., & Roelvink, D. (2016). Modeling centuries of estuarine morphodynamics in the Western Scheldt estuary. *Geophysical Research Letters*, 43(8), 3839-3847.
- Deltares (2014). Delft3D-FLOW, User manual. *3D/2D modelling suite for integral water solutions*, Hydro-Morphodynamics. Deltares
- Fan, J., & Morris, G. L. (1992). Reservoir sedimentation. II: Reservoir desiltation and long-term storage capacity. *Journal of Hydraulic Engineering*, 118(3), 370-384.
- Garcia, M. H., Editor (2008). *Sedimentation Engineering: Theory, Measurements, Modeling, and Practice (Manuals and Reports on Engineering Practice No. 110) (ASCE Manual and Reports on Engineering Practice)*. American Society of Civil Engineers, Reston.
- Giardino, A., Elias, E., Arunakumar, A., & Karunakar, K. (2014). Tidal modelling in the Gulf of Khambhat based on a numerical and analytical approach. *Indian Journal of Geo-Marine Sciences*, 1257-1263.
- Giardino, A., Schrijvershof, R., Nederhoff, C. M., de Vroeg, H., Brière, C., Tonnon, P. K., & Schellekens, J. (2018). A quantitative assessment of human interventions and climate change on the West African sediment budget. *Ocean & Coastal Management*, 156, 249-265.
- Hoitink, A. J. F., Wang, Z. B., Vermeulen, B., Huismans, Y., & Kästner, K. (2017). Tidal controls on river delta morphology. *Nature Geoscience*, 10(9), 637.
- Manning, R., Griffith, J. P., Pigot, T. F., & Vernon-Harcourt, L. F. (1890). *On the flow of water in open channels and pipes (Vol. 20)*. Transactions of the Institution of Civil Engineers of Ireland.
- Montesdeoca, S. (2018). Personal communication, ELECAUSTRO S.A.
- Partheniades, E. (1964). *A summary of the present knowledge of the behavior of fine sediments in estuaries*. Hydrodynamics Lab., Department of Civil and Sanitary Engineering, Massachusetts Inst. of Technology.
- Savenije, H. H. (2006). *Salinity and tides in alluvial estuaries*. Elsevier.
- Sutherland, J., Peet, A. H., & Soulsby, R. (2004). Evaluating the performance of morphological models. *Coastal engineering*, 51(8-9), 917-939.
- Van der Wegen, M., & Roelvink, J. A. (2012). Reproduction of estuarine bathymetry by means of a process-based model: Western Scheldt case study, the Netherlands. *Geomorphology*, 179, 152-167.
- Van Rijn, L. C., Walstra, D. J. R., Grasmeijer, B., Sutherland, J., Pan, S., & Sierra, J. P. (2003). The predictability of cross-shore bed evolution of sandy beaches at the time scale of storms and seasons using process-based profile models. *Coastal Engineering*, 47(3), 295-327.
- Van Rijn, L. C. (1990). *Principles of fluid flow and surface waves in rivers, estuaries, seas and oceans* (Vol. 12). Amsterdam, The Netherlands: Aqua Publications.
- Winterwerp, J. C. (2013). On the response of tidal rivers to deepening and narrowing. *Risks for a Regime Shift Towards Hyper-turbid Conditions*, 105.